Analysis on Electrolytic Behavior of Aluminium Dodecaboride/Alumina (AlB_{12}/Al_2O_3) Composite Ceramic Powder

Chao Wang[1]*, Berkley Yiu[2], Mengge Dong[3], Xiaozhou Cao[3]*, and Xiangxin Xue[3]*

[1]Department of Mechanical Engineering, The University of Texas at Dallas, Richardson, TX, 75080, USA
[2]Plano Senior High School, Plano, TX, 75075, USA
[3]School of Metallurgy, Northeastern University, Shenyang, Liaoning, 110819, China

Chao Wang, Berkley Yiu, and Mengge Dong made an equal contribution.

*Corresponding author. E-mail: wang.chao@utdallas.edu,caoxz@smm.neu.edu.cn,xuexx@mail.neu.edu.cn

Abstract

Although the excellent properties of borides have attracted the attention of the industry, their limited preparation process and difficult-to-remove impurities have prevented them from exerting their full effectiveness. However, it is very difficult to separate AlB_{12} and Al_2O_3 prepared by self-propagating high temperature synthesis. This study is the first time to separate the two by electrolysis process and observe their electrolytic behavior. The results show that Al_2O_3 is converted into micron-sized aluminum during the electrolysis process, while AlB_{12} still exists intact. This result provides a novel idea for the future purification of borides containing Al_2O_3 impurities.

Keywords: Boride; Aluminum Dodecaboride; Self-propagating high-temperature synthesis (SHS); Electrolysis

Introduction

Ceramic materials refer to a class of inorganic non-metallic materials made from natural or synthetic compounds through forming and high-temperature sintering (1-4). It has the advantages of high melting point, high hardness, high wear resistance, and oxidation resistance . It can be used as structural material and tool material (5-8). Due to ceramics also have some special properties, it can also be used as a functional material (9-12).

As one of the modern high-tech ceramic materials, boride ceramics are used as hard tool materials, abrasives, alloy additives, wear-resistant and corrosion-resistant parts due to their high melting point, high hardness, high oxidation resistance and high wear resistance (13-17). This kind

of material has excellent electrical properties and has been highly valued as an inert electrode material and high temperature electrical material.

Metal borides are interstitial phase compounds, and their chemical bond composition is relatively complex (18, 19). At the same time, they include one or more of MM metal bond, BB covalent bond and BM ionic bond. This determines that the boride has a variety of characteristics from the microscopic level. At present, the application of boride ceramic in the coating field are binary, ternary borides and multi-borides, etc.; the main preparation technologies include APS (atmospheric plasma spraying) (20), HVOF (supersonic flame spraying) (21), plasma cladding (22), laser cladding (23), argon arc cladding (24), induction cladding (25), vapor deposition (26), magnetron sputtering (27), etc.

AlB_{12} has the same icosahedral B_{12} structure as B_4C (15, 28, 29). This unique rigid and open boron atom frame structure determines that AlB_{12} has the characteristics of high melting point, low specific gravity, high hardness, and wear resistance. These characteristics are like those of B_4C. The characteristics are extremely similar, which also makes it as broad as B_4C in grinding and weaponry. AlB_{12} has very strong corrosion resistance, and only hot nitric acid can dissolve it. The high temperature resistance of AlB_{12} makes it possible to be used in military equipment such as rocket nozzles (7, 30).

The preparation process of AlB_{12} mainly includes: (1) Thermal shock sintering using Al and B_2O_3 as raw materials (31); (2) Vacuum reaction sintering using Al and B as raw materials (32); (3) Molten salt assisted synthesis using KBF_4 and aluminum as raw materials (33). These processes have obvious defects such as: complex process, expensive raw materials, extremely low output, and impurities. As a primary impurity and accompanying products, α-Al_2O_3 has stable chemical and physical properties and difficult to remove, making the purity of AlB_{12} unable to be improved.

In previous studies, it was found that AlB_{12} can be prepared by self-propagating reaction, but the accompanying existence of Al_2O_3 cannot be avoided and removed at all (7, 29, 30). Self-propagating high-temperature synthesis (SHS), also known as combustion synthesis, uses the heat released by the combustion reaction of the original chemical reaction raw materials to make the chemical reaction process spontaneously and continuously, to obtain a new type of material synthesis method with a specified composition and structure product.

Electrolytic aluminum is a high-temperature process that can consume large amounts of alumina (17, 34, 35). In the electrolytic cell, the melted cryolite is the solvent, the alumina is dissolved in it as the solute, the carbon body is used as the anode, and the aluminum liquid is used as the cathode. After a strong direct current is applied, it is carried out on the two poles of the electrolytic cell at 950 to 970 °C. Electrochemical reaction, aluminum liquid is obtained at the cathode, and gas is obtained at the anode, namely electrolysis.

Reaction equation at cell:

$$2Al_2O_3 = 4Al + 3O_2$$

Reaction at anode：

$$2O_2^- - 4e^- = O_2 \uparrow$$

Reaction at cathode：

$$Al^{3+} + 3e^- = Al$$

In this study, for the first time, the aluminum electrolysis process was used to observe the aluminum electrolysis behavior with AlB_{12}/Al_2O_3 composite ceramic powder prepared by self-propagating high temperature synthesis as the solute.

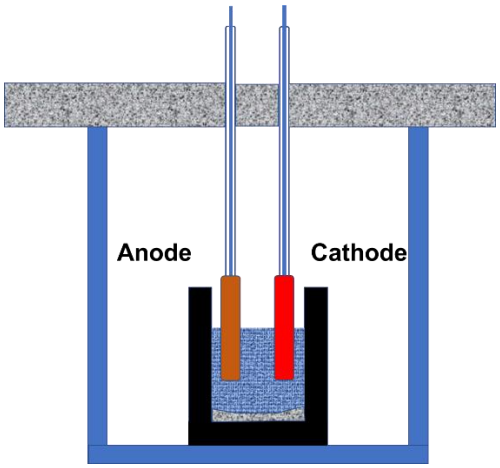

Figure 1 Experiment Setup of electrolytic cell

Materials and Methodology

The starting materials used in this research were Al powder (purity＞99% Al, average particle size 50 μm, provided by Dandong Chemical Research Institute, Dandong, China), B_2O_3 powder (purity＞99%, average particle size 96 μm, provided by Dandong Chemical Research Institute, Dandong, China). Analytical reagent cryolite (Na_3AlF_6, >99%) ,aluminum fluoride (AlF_3, >99%), and calcium fluoride (CaF_2, >99%) came from Xiya Reagent Company, Chengdu.

The steps used in the self-propagating process to synthesize AlB_{12}/Al_2O_3 ceramic powder are as follows: (1) Weigh a certain amount (45 wt.% Al and 55 wt.% B_2O_3) of the original material powder, place it in the ball milling tank, and mix the ball mill for 2 hours. (2) Intercept the resistance wire and connect it to the two poles of the self-propagating device and place the material under Ar with one end close to the resistance wire. (3) Start the ignition device and slowly increase the current. When the pointer fluctuates sharply, reduce the current and keep the current increasing steadily. Finally, the resistance wire will reach a molten state when the material is induced to burn, and the current is turned off. (4) The reaction product is pulverized and sieved with 160 meshes, and samples under the sieve are sampled for detection and analysis.

Add 15% of its mass of AlF_3 to cryolite Na_3AlF_6 (3NaF: AlF_3) so that the molecular ratio of NaF to AlF_3 in the cryolite is less than 3:1 and greater than 2.1:1, and then add 10% of its mass to CaF_2, 800 g electrolyte material is placed in the electrolytic cell, the material of the electrolytic cell is high-purity graphite, the temperature of the electrolytic cell is 20~100 °C higher than the melting point of the electrolyte mixture; add 10 g AlB_{12}/Al_2O_3 mixed powder into the electrolytic cell and mix it evenly, Obtain the molten mixed electrolyte, insert a high-purity graphite cylinder as the anode into the electrolytic cell, and energize the electrolytic cell. The electrolysis voltage is 8 V, the electrolysis current is 20 A, the current density is 0.5 A/cm^2, the electrolysis time is 4 h, every 25 min then add 10 g AlB_{12}/Al_2O_3 mixed powder to the electrolytic cell. During the electrolysis process, the electrolysis product located at the cathode is taken out and analyzed and studied.

The phase analysis of the synthesized powder was carried out using an X-ray diffractometer (XRD, X'Pert Pro MRD, Netherlands) with a Philips diffractometer using Cu Ka. The microstructure of the electrolysis product and elements analysis were investigated using a scanning electron microscope with EDS detector (SEM, S-3400N, Japan).

Results and Discussion

Figure 2 is the X-ray diffraction pattern of Al and B_2O_3 prepared under argon conditions. Note that AlB_{12} and Al_2O_3 are synthesized by SHS process. In the previous research, the high temperature process will promote the conversion of alumina phase into Alpha-alumina (α-Al_2O_3) which has excellent chemical and physical stability.

In the self-propagating reaction, the following chemical reactions mainly occur:

$$13Al+6B_2O_3 \rightarrow AlB_{12}+6Al_2O_3$$

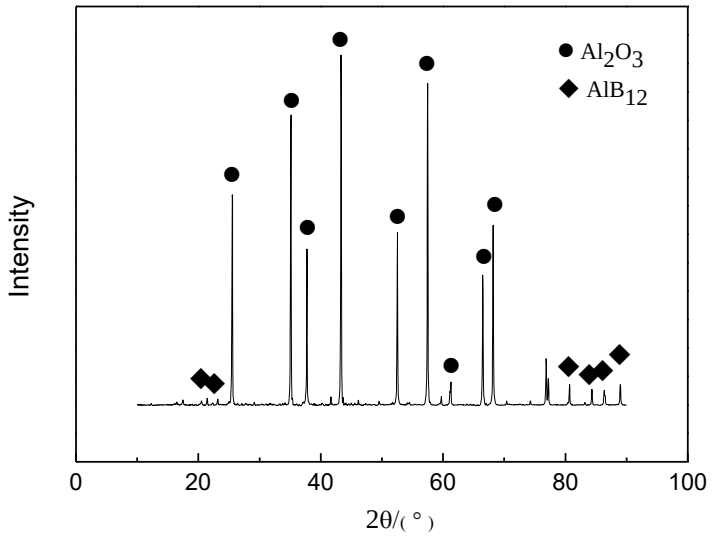

Figure 2 XRD patterns of fabrication AlB_{12}/Al_2O_3

Figure 3 shows the photo of the electrolysis product and the energy spectrum of the element of Al, B, and O. The energy spectrum of aluminum element shows that there is a large amount of aluminum element in a specific area. The gradual enrichment of Al element indicates that Al is formed, and Al_2O_3 is transforming to Al. In the area with B element, there is mostly Al element but no O element. , Indicating that AlB_{12} is in Al. Such element distribution shows that after the electrolysis process, Al_2O_3 changes to aluminum, but AlB_{12} still remains alone without any change.

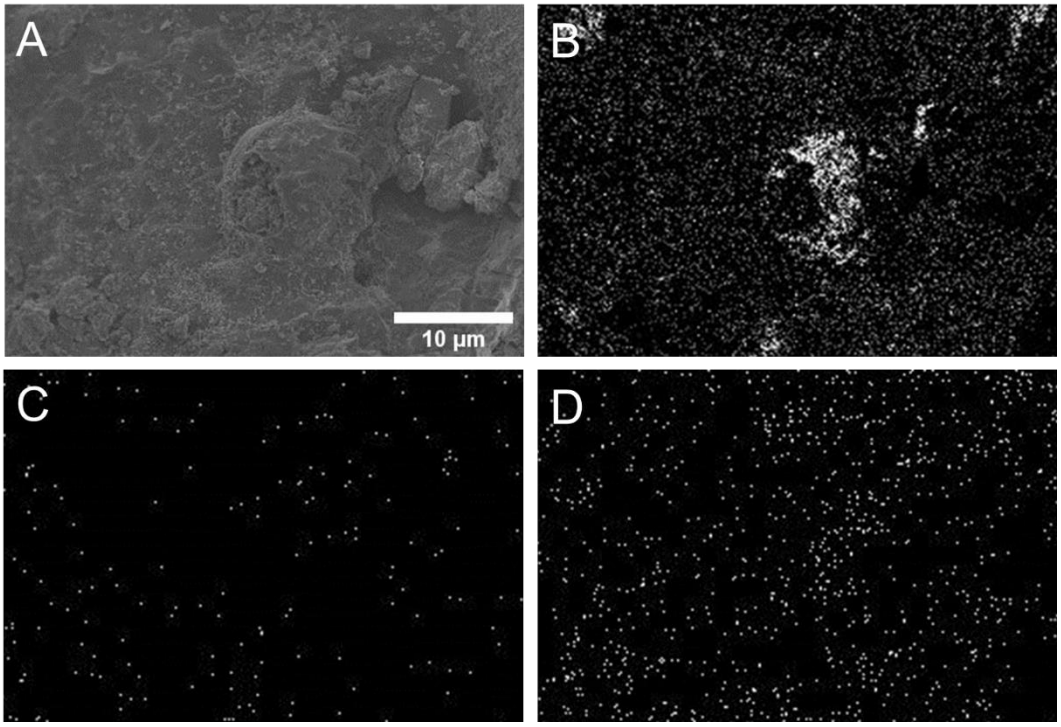

Figure 3 Image of electrolysis product (A) and EDS mapping analysis: (B) Al, (C) B, (D)O.

Figure 4 shows the aluminum in the electrolysis product. The shape of the entire aluminum is spherical. The large aluminum ball is composed of many micron-scales spherical aluminum, as it is shown in the SEM image of Figure 4 (B). The diameter of the nano-scale aluminum ball is 30~80 μm. The scale of Al is in the micron level, which may be due to the presence of AlB_{12}, which makes the composite ceramic powder increase the resistance effect during the electrolysis process, making the electrolysis behavior not continuous. Moreover, the presence of aluminum indicates that the AlB_{12}/Al_2O_3 composite ceramic powder has aluminum electrolysis during the electrolysis process, and α-Al_2O_3 has been transformed into Al. This experimental phenomenon indicates that the composite ceramic powder of AlB_{12}/Al_2O_3 can be electrolyzed.

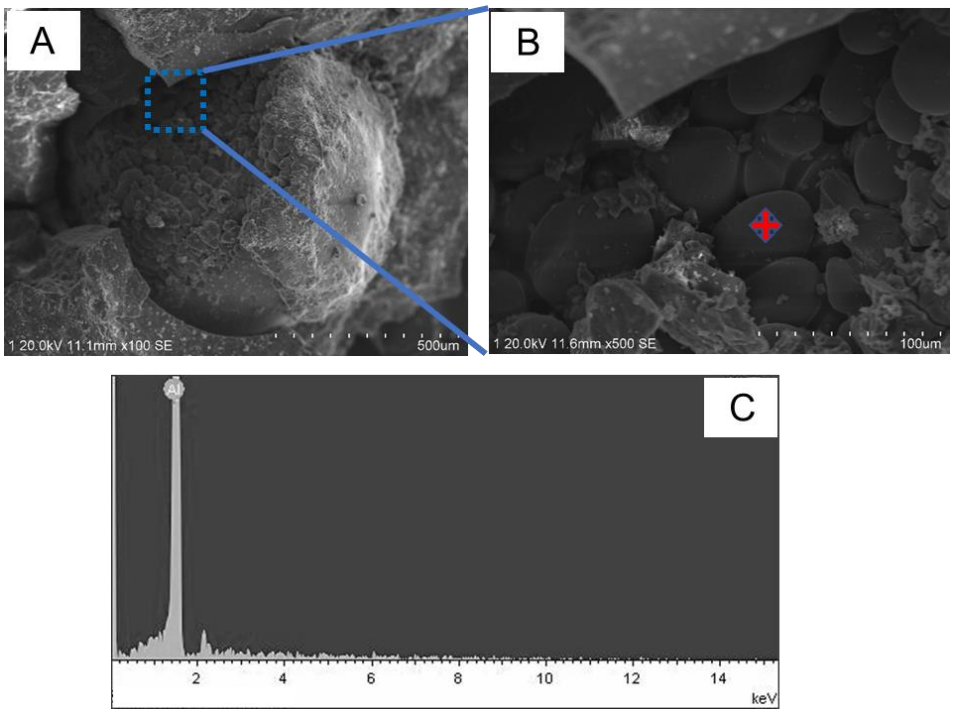

Figure 4 Image of Aluminum and EDS analysis: (A) Al image, (B) zoom in (A) area, (C) Al spectrum

Summary

For the first time, AlB_{12}/Al_2O_3 powder was synthesized by self-propagating high temperature, and electrolysis was conducted on it. The research results show that AlB_{12}/Al_2O_3 composite ceramic powder was successfully prepared by SHS. After electrolysis, micron-sized Al balls appeared, and AlB_{12} still exists in electrolysis product. This research provides novel ideas for the future preparation of high-purity AlB_{12} through the aluminum electrolysis process, which may be extended to other ceramic powders which associated with Al_2O_3.

Notes

The authors declare that they have no competing financial interest.

Acknowledgements

This work was supported by the fundamental, scientific-research business resources of the central universities (award # N10060200).

References

1. X. Cao *et al.*, Effect of Ni addition on pressureless sintering of tungsten diboride. *International Journal of Refractory Metals and Hard Materials* **41**, 597-602 (2013).
2. C. Wang *et al.*, A New Method of Fabricating AlN-TiB_2 Composite Ceramics. *Materials and manufacturing processes* **28**, 953-956 (2013).
3. X. Cao, C. Wang, X. Xue, H. Yang, Preparation of tungsten boride ceramic by pressureless sintering. *Journal of Inorganic Materials* **29**, 498-502 (2014).
4. X. Cao, C. Wang, X. Xue, G. Cheng, Effect of ti addition on the residual aluminium content and mechanical properties of the B_4C-al composites produced by vacuum infiltration. *Archives of Metallurgy and Materials* **60**, 2493-2398 (2015).
5. B. R. Golla, A. Mukhopadhyay, B. Basu, S. K. Thimmappa, Review on ultra-high temperature boride ceramics. *Progress in Materials Science* **111**, 100651 (2020).
6. P. Loganathan, A. Gnanavelbabu, K. Rajkumar, S. Ayyanar (2020) A comparative study of solid lubricant types on the microstructure and mechanical behaviour of AA7075-zirconium boride aerospace composites. in *IOP Conference Series: Materials Science and Engineering* (IOP Publishing), p 012001.
7. C. Wang *et al.*, Theoretical Calculation of Self-Propagating High-Temperature Synthesis (SHS) Preparation of AlB_{12}. https://doi.org/10.26434/chemrxiv.13591427.v1. (2021).
8. C. Wang *et al.*, Research on Thermal Neutron Shielding Performance of TiB_2-Al Composite Materials. *ChemRxiv* https://doi.org/10.26434/chemrxiv.13611725.v1 (2021).
9. C. Wang, X. Xue, X. Cao, H. Yang, Effect of BN Addition on Mechanical Properties and Microstructure of TiB_2-Al Composites. *Journal of Northeastern University (Natural Science)*, 19 (2012).
10. C. Wang, X. Xue, X. Cao, H. Yang, G. Cheng, The effect of Ti addition on the microstructure and fracture toughness of BN-Al composite materials synthesized by vacuum infiltration. *Archives of Metallurgy and Materials* **58**, 509-512 (2013).
11. C. Wang, J. Zhang, X. X. Xue, X. Z. Cao (2013) Fabrication B-Ni-Al Shielding Materials by Vacuum Metal Infiltration. in *Advanced Materials Research* (Trans Tech Publ), pp 410-413.
12. C. Wang *et al.*, Research Progress on Aluminum-Boron Compounds (Al-B) and Its Composite Materials. *Bulletin of the Chinese Ceramic Society*, 26 (2013).
13. E. Clougherty, R. Pober, L. Kaufman (1968) Synthesis of oxidation resistant metal diboride composites. (ManLabs., Inc., Cambridge, Mass.).
14. V. I. Matkovich, *Boron and refractory borides* (Springer, 1977).
15. D. Gosset, M. Guery, B. Kryger (1991) Thermal properties of some boron‐rich compounds ("BnC" and AlB_{12}). in *AIP Conference Proceedings* (American Institute of Physics), pp 380-383.
16. X. Luo *et al.*, Influence of metallic additives on densification behaviour of hot-pressed TiB_2. *Light Metals*, 1151-1155 (2009).
17. X. Cao *et al.* (2011) High temperature electrochemical synthesis of tungsten boride from molten salt. in *Advanced Materials Research* (Trans Tech Publ), pp 463-466.
18. M. Dong *et al.*, A novel comprehensive utilization of vanadium slag: as gamma ray shielding material. *Journal of hazardous materials* **318**, 751-757 (2016).
19. M. Mahmoudi *et al.*, Three-Dimensional Printing of Ceramics through “Carving” a Gel and “Filling in” the Precursor Polymer. *ACS Applied Materials & Interfaces* **12**, 31984-31991 (2020).
20. Y. Zeng, S. W. Lee, C. Ding, Study on plasma sprayed boron carbide coating. *Journal of thermal spray technology* **11**, 129-133 (2002).

21. M. Ksiazek, L. Boron, A. Tchorz, Microstructure, Mechanical Properties and Wear Behavior of High-Velocity Oxygen-Fuel (HVOF) Sprayed (Cr3C2-NiCr+ Al) Composite Coating on Ductile Cast Iron. *Coatings* **9**, 840 (2019).
22. C.-H. Tian *et al.*, Effect of boron on microstructure and performance of wear-resisting steel plate prepared by plasma cladding. *Transactions of Materials and Heat Treatment* **32**, 138-142 (2011).
23. J. Y. Aguilar-Hurtado *et al.*, Boron addition in a non-equiatomic Fe50Mn30Co10Cr10 alloy manufactured by laser cladding: Microstructure and wear abrasive resistance. *Applied Surface Science* **515**, 146084 (2020).
24. H. Wang *et al.*, Microstructure and mechanical properties of molybdenum–iron–boron–chromium cladding using argon arc welding. *Materials Science and Technology* **32**, 1694-1701 (2016).
25. B. Huang, Y. Gao, P. Chen, W. Xiong, J. Tang, Microstructure and properties of Ni+ B4C/Ti coatings by high-frequency induction cladding. *Surface Innovations* **7**, 59-67 (2018).
26. A. O. Sezer, J. Brand, Chemical vapor deposition of boron carbide. *Materials Science and Engineering: B* **79**, 191-202 (2001).
27. T. Hu *et al.*, Structures and properties of disordered boron carbide coatings generated by magnetron sputtering. *Thin Solid Films* **332**, 80-86 (1998).
28. I. Higashi, Crystal chemistry of α-AlB_{12} and γ-AlB_{12}. *Journal of solid state chemistry* **154**, 168-176 (2000).
29. C. Wang *et al.* (2014) Elementary research on preparation of AlB_{12} powder by self-propagating high-temperature synthesis (SHS). in *Materials Science Forum* (Trans Tech Publ), pp 365-369.
30. C. Wang *et al.*, Preparation of AlB_{12} Powder by Self-Propagating High-Temperature Synthesis (SHS). https://doi.org/10.26434/chemrxiv.13591313.v1. (2021).
31. D. Wang, H. Yang, Y. Zhang, X. Xue, Preparation and characterization of alb 12 powder. *Journal of the Chinese ceramic society* **36**, 1443-1449 (2008).
32. D.-s. WANG, X.-x. XUE, Lab Preparation of AlB_ (12) Powder. *Bulletin of the Chinese Ceramic Society*, 02 (2008).
33. N. El-Mahallawy, M. A. Taha, A. E. Jarfors, H. Fredriksson, On the reaction between aluminium, K2TiF6 and KBF4. *Journal of alloys and compounds* **292**, 221-229 (1999).
34. X. Hu *et al.* (2007) Nd_2O_3 Solubility in NdF_3-LiF-Nd_2O_3 Melts. in *Proceedings of NGCWP 2007*.
35. W. Tao *et al.* (2009) Finite element analysis of thermo-electric coupled field in 400kA large-scale aluminum reduction cell. in *2009 World Non-Grid-Connected Wind Power and Energy Conference* (IEEE), pp 1-4.